JOURNAL OF VIROLOGY, Dec. 1995, p. 8084–8088 Vol. 69, No. 12
0022-538X/95/$04.00+0

Susceptibility and Signs Associated with Mouse Adenovirus Type 1 Infection of Adult Outbred Swiss Mice

SUSAN C. KRING,[1] CHRISTOPHER S. KING,[2] AND KATHERINE R. SPINDLER[1]*

Department of Genetics[1] and Office of the Vice President for Research,[2] University of Georgia, Athens, Georgia 30602

Received 24 April 1995/Accepted 7 September 1995

Adult Swiss outbred mice from two sources had a nearly 6,000-fold difference in susceptibility to mouse adenovirus type 1-induced disease. This difference was not attributable to differential organ tropism. Signs associated with mouse adenovirus type 1 infection that have not been previously reported are described at the clinical, gross pathological, and histological levels.

Human adenoviruses have been used to study DNA replication, mRNA splicing, gene transactivation, and host cell protein-viral protein interactions. Because of their species specificity, the molecular pathogenesis of human adenoviruses cannot be fully analyzed in an animal model. Studies of mouse adenovirus type 1 (MAV-1) infections have been reported but have failed to examine the molecular basis for pathogenesis of the virus. We are using MAV-1 infection of mice as a model system to understand adenoviral pathogenesis.

Mice lacking full immunocompetency are highly susceptible to MAV-1 infection (13). Mortality is seen from 3 to 10 days postinfection (p.i.) (2, 7) in newborn and suckling mice and is associated with necrosis of the kidney, heart (2, 6, 7, 9), spleen, brain (7), adrenal glands, pancreas, liver, and intestines (9). Salivary glands and the brown fat are also affected but to a lesser extent (6, 9). Signs of disease include ruffled coat, lethargy, runting, and terminal burrowing into the cage bedding (7, 9, 13, 18). Adult mice carrying the severe combined immune deficiency mutation and infected with MAV-1 display additional signs of hunching, unsteady gait, and poor feeding; histopathologic changes in the liver, adrenal glands, and spleen; and mortality between 6 and 18 days p.i. (10). Athymic, *nu/nu* mice infected with MAV-1 display a lethal wasting disease characterized by hunched posture, drastic weight loss, and scaling skin, accompanied by pathological lesions of the duodenum (19). Mortality is often delayed, occurring between 2 and 134 days p.i. at doses between 10^2 and 10^7 PFU. Resistance to clinical disease is acquired between 15 and 27 days of age (18). This corresponds to the time of mouse immune system maturation between 14 and 21 days of age (5, 16).

MAV-1 infection of adult immunocompetent mice is most often associated with a subclinical, persistent infection (13). Persistence is manifested by high serum antibody titers (7, 17) and prolonged viruria (up to 24 months p.i.) in the absence of clinical signs (6, 17). A viremic state has been demonstrated from 4 to 10 days p.i. (17). Virus is disseminated throughout many organs at up to 14 days p.i., with the highest titers at 10 days p.i. in the spleen (17). In a separate study, virus was detected in the kidney for up to 70 days p.i. (4). There have been only two reports of clinical disease associated with MAV-1 infection of adult immunocompetent mice at high doses. Winters et al. (20) reported physical inactivity, hunched posture and puffed fur at doses of 10^6 to 10^7 PFU. van der Veen and Mes (17) reported the same signs plus decreased food consumption and swelling of the spleen and peripheral lymph nodes at a dose of 2,000 50% tissue culture infective doses.

In this report, we describe the differential susceptibility of two outbred mouse strains to MAV-1-induced disease, describe new signs associated with disease in immunocompetent mice, and describe the level of involvement of different organs on the basis of the presence of associated viral DNA, gross pathological findings, and histological examination.

Four-week-old male CD-1 Swiss mice from Charles River Laboratories (CD-1) were inoculated intraperitoneally (i.p.) with 10-fold dilutions of virus from 10^1 to 10^6 PFU of MAV-1 (cultured and titered on L929 cells) per animal. Uninfected animals served as controls. The 50% lethal dose (LD_{50}) was equivalent to 10^5 PFU, as determined by the method of Reed and Muench (12). Previous studies (1) had indicated a significantly lower LD_{50} for NIH Swiss outbred mice from Harlan Sprague Dawley, Inc. (NIHS). CD-1 and NIHS mice were then compared concurrently for their susceptibility to MAV-1-induced disease in a dosage response experiment. Four-week-old mice from both suppliers were obtained and infected i.p. with 10-fold dilutions of MAV-1 from 10^1 to 10^5 PFU per animal (Table 1). NIHS mice succumbed to the infection with an LD_{50} equivalent to 17 PFU, nearly 6,000-fold lower than that for CD-1 mice ($LD_{50} > 10^5$ PFU). Additionally, some mice of both strains displayed clinical signs of neurological disease which had not been previously reported for MAV-1 infection of adult immunocompetent mice. A total of 2 of the 29 CD-1 mice and 12 of the 30 NIHS mice developed signs ranging from mild ataxia to hyperreflexia to flaccid paralysis. Three of the ataxic NIHS mice recovered but were runted.

To investigate the difference in susceptibility of the two mouse strains to MAV-1-induced disease, mice were inoculated i.p. with virus at doses bracketing their respective LD_{50}. Control mice were inoculated with conditioned cell culture media. The mice were observed for overt signs of disease and euthanized, and necropsies were performed. Organ samples were analyzed for the presence of viral DNA by PCR amplification and dot blot hybridization and for tissue damage by histology.

Mice were observed several times daily, and signs were recorded. Onset of clinical signs was strain and dose dependent. Onset occurred 3 days p.i. for CD-1 mice receiving 10^6 PFU and between 4 and 5 days p.i. for those receiving 10^5 PFU. Onset in NIHS mice occurred between 4 and 9 days p.i. for mice receiving 10^2 PFU and between 8 and 12 days p.i. for those receiving 10^1 PFU. Initial clinical signs became apparent

* Corresponding author. Mailing address: Department of Genetics, Life Sciences, University of Georgia, Athens, GA 30602-7223. Phone: (706) 542-8395. Fax: (706) 542-3910. Electronic mail address: spindler@uga.cc.uga.edu.

TABLE 1. Differential susceptibility of outbred Swiss mouse strains to MAV-1 infection

Infectious dose[a] (PFU)	Outbred Swiss mouse strain			
	NIHS		CD-1	
	No. survived/ no. infected	Day of death p.i.	No. survived/ no. infected	Day of death p.i.
10^5	0/6	3, 3, 3, 3, 5, 7	5/6	4
10^4	1/6	5, 6, 6, 7, 11[b]	5/6	7
10^3	0/6	7[b], 7, 7, 8[b], 8, 9[b]	5/5	
10^2	3/6	9, 9, 10[b]	5/6	9[b]
10^1	2/6	11[b], 11[b], 11, 12[b]	5/6	11[b]
None	6/6		7/7	

[a] Mice were injected i.p. with the indicated dose.
[b] Mice exhibiting signs of hyperreflexia or flaccid paralysis.

as a ruffled coat and mild ataxia with the tail held rigidly. The gait of affected mice appeared mechanical and exaggerated. Hyperesthesia was noted when mice were touched or stroked. In most cases, clinical signs progressed over the ensuing 24 to 48 h to total flaccid paralysis with hyperpnea, abdominal breathing, and distention of the urinary bladder. Corneal reflexes were exaggerated. Mice in intermediate stages showed varying signs such as posterior paresis, ataxia, hyperreflexia, and paraphimosis. Some mice died acutely, without clinical signs being observed. One ataxic mouse with hyperpnea and paraphimosis showed no other clinical signs following 7 days of recovery. Both CD-1 and NIHS mice exhibited the above signs to approximately the same degree. The lower doses of inoculum resulted only in a delay of onset. Progressive neurological signs associated with MAV-1 infection have not been previously reported, although Heck et al. and Margolis et al. (7, 9) report intranuclear inclusions in the endothelial cells of blood vessels in all major divisions of the brain and focal involvement of Purkinje's cells of the cerebellum (7) in MAV-1-infected suckling mice. To rule out possible involvement of secondary infections, serum samples from mock- and MAV-1-infected CD-1 and NIHS animals were analyzed. Samples were negative for antibodies against coronavirus, lymphocytic choriomeningitis virus, parvovirus, reovirus, Theiler's murine encephalomyelitis virus, and polyomavirus. Serum levels of lactate dehydrogenase in mock- and MAV-1-infected mice did not differ from each other, were within the range of published norms (14), and did not suggest infection by lactate dehydrogenase elevating virus.

The clinical signs listed above were grouped by level of severity into five classes, 0 to 4 (Table 2). Mice with three or more class 3 signs or one or more class 4 signs were considered moribund and were euthanized. All surviving mice in the study were euthanized by 21 days p.i.

Necropsy of affected mice revealed runting, dehydration, and involution of the thymuses. The gastrointestinal tracts were usually empty, and segmental enteritis of the distal duodenum and jejunum was occasionally observed. Testes were intra-abdominal. Control animals and infected mice with no clinical signs appeared normal.

DNA samples were prepared from various organs (bowel, pancreas, spleen, adrenal gland, kidney, liver, lung, heart, brain, and spinal cord) of all mice and were analyzed for the presence of MAV-1 DNA by PCR amplification and dot blot hybridization (Table 2). Additionally, DNA samples were prepared from the Peyer's patches from regions of segmental enteritis and the testes of several mice. Organ samples from uninfected animals were used as controls. DNA was extracted from organ samples by incubation overnight in lysis buffer (8) followed by phenol-chloroform extraction and ethanol precipitation. Virus was added to duplicate samples from an uninfected mouse of each strain prior to lysis as a standard for the sensitivity of detection. Control organ samples were spiked with 500 PFU of virus, which corresponds to 5×10^5 particles, based on a ratio of 1,000 particles per PFU (14a). Samples diluted 1:160 were used for PCR amplification and contained 0.5 μg of DNA corresponding to 10^5 mouse genomes and 3,125 virus particles per sample. Primers (5′ TGTGCCTGCTTCTA CTC 3′ and 5′ ACGCTGCTGTTAGAAAC 3′ were made to amplify a 410-bp region of MAV-1 early region 3 (1a, 11). As an internal control for integrity of the DNA and the amplification reactions, primers designed to amplify a 246-bp region of the mouse myogenin gene were included with each sample (5′ TTACGTCCATCGTGGACAGC 3′ and 5′ TGGGCTGG GTGTTAGCCTTA 3′) (3). To quantitate the amount of virus in each sample that was positive in the PCR assay, equivalent amounts of DNA from each sample were dotted onto nitrocellulose filters. The filters were probed with radioactively labeled DNA corresponding to 0 to 16.5 map units of the MAV-1 genome and separately with an oligonucleotide complementary to the mouse 18S rRNA gene (15). The signal was detected by phosphorimetry and quantitated with ImageQuant software (Molecular Dynamics). The amount of viral DNA was normalized to the rRNA signal in each sample.

To determine whether there was a difference in the level of infection between the two mouse strains, a Mann-Whitney rank sum test was performed for each organ with SigmaStat software. These tests indicated a significant difference ($P = 0.04$) in the level of infection of the adrenal gland between CD-1 (higher level) and NIHS mice. However, the adrenal gland has among the lowest virus levels of the organs tested. There were no other significant differences in the organ tropism of the virus between the two strains of mice that could account for the vast difference in their LD_{50} (Table 2).

Additionally, a repeated-measures analysis of variance on ranks was performed, excluding the spinal cord data. This was followed by a Student-Newman-Keuls multiple pairwise comparison to rank which organs had the highest virus levels. The analysis was performed on the normalized values for organs of the mice of each strain separately and with normalized values for the two strains combined. In all three cases, the spleens had higher virus levels than the brains ($P < 0.05$), which had higher levels than each of the other organs ($P < 0.05$).

Tissue specimens from all of the organs used to prepare DNA samples and additionally from the stomach, small bowel, large bowel, cecum, testes, skeletal muscle, skin, lymph nodes, salivary glands, and eye were fixed in 10% neutral buffered formalin. Paraffin-embedded 3-μm sections were prepared and stained with Gill's hematoxylin II and eosin (Surgipath). The brain and spinal cord exhibited a vascularly oriented encephalomyelitis, with multifocal acute endothelial necrosis (Fig. 1A), perivascular gliosis with necrosis, and petechial hemorrhage (Fig. 1B and C). The spinal cord lesions correlate with the clinical signs including rigid tail carriage, hypermetria, paraphimosis, and distension of the urinary bladder. Necrosis and hemorrhage were observed in the cerebellum, which correlates with the observed ataxia. A generalized lymphocytic necrosis was noted in the spleen, lymph nodes, and thymus. In some intestinal sections, there was severe epithelial necrosis of the villi and hemorrhage in the mucosa and submucosa (Fig. 1D). Intranuclear inclusions were not observed in tissue sections from infected mice of either strain. There was no difference in

TABLE 2. PCR and dot blot hybridization analyses of viral DNA in the organs of MAV-1-infected mice with different signs[a]

Mouse strain, dose, and designation[b]	Level or presence of MAV-1 in organ									
	Bowel	Pancreas	Spleen	Adrenal gland	Kidney	Liver	Lung	Heart	Brain	Spinal cord
NIHS										
10^2 PFU										
Class 1	0.14	0.00	0.16	−	0.00	0.08	0.06	0.00	0.06	+
Class 2	−	−	0.22	−	0.06	0.02	−	0.00	−	0.00
Class 2	−	−	0.19	−	−	−	−	−	0.01	+
Class 2	−	−	0.27	0.02	0.10	0.00	−	0.02	0.08	+
Class 3	−	−	0.04	0.00	0.00	0.02	−	0.02	ND[c]	0.00
Class 3	−	0.00	0.08	−	0.01	0.01	0.79	0.04	0.02	0.00
E9	0.00	0.00	0.15	0.11	0.04	0.09	0.09	0.03	0.04	0.19
E9	−	0.59	−	−	−	0.02	−	0.01	0.10	−
E8	0.05	0.00	0.54	0.00	0.00	0.00	−	0.00	0.13	0.32
E8	0.00	0.77	0.54	0.04	0.06	0.04	0.13	0.05	0.03	0.02
10^1 PFU										
Class 0	−	−	0.03	−	0.06	−	−	−	0.00	−
Class 1	−	−	0.13	−	−	−	−	0.04	−	−
E13	0.53	0.32	0.00	0.00	0.01	0.04	0.24	0.09	2.48	1.91
E12	1.05	9.19	0.67	−	0.11	0.31	0.31	0.04	0.92	1.20
E12	0.05	0.00	0.27	0.00	0.00	0.05	0.85	0.39	1.61	3.17
E12	0.21	0.20	0.14	0.00	0.07	0.66	0.35	0.07	0.71	0.47
E13	0.80	0.09	0.27	0.24	0.33	0.05	0.18	0.16	0.83	+
D12	0.00	0.00	0.36	0.17	0.00	0.06	0.00	0.00	0.09	0.17
D12	0.00	0.00	0.00	0.06	−	0.00	0.49	0.00	0.24	+
D12	0.74	0.50	0.61	0.00	0.05	0.00	0.02	0.03	0.37	+
CD-1										
10^6 PFU[d]										
Class 0	−	−	−	−	−	−	−	−	−	−
E3	0.93	7.18	0.74	0.05	0.11	0.02	0.19	0.28	0.50	+
E3	0.27	0.00	0.41	0.05	−	0.02	−	0.05	0.05	0.13
D3	0.68	1.42	0.60	0.27	0.11	0.03	0.98	0.06	0.31	ND
D3	0.44	0.00	0.71	0.12	0.03	0.03	−	0.11	0.48	+
D3	2.67	0.00	0.05	0.10	0.00	0.06	0.40	0.06	0.60	+
D3	−	0.00	0.21	1.23	0.04	0.20	1.02	0.00	0.95	+
D3	0.94	0.00	0.28	0.00	0.00	−	0.00	0.04	0.04	ND
D3	0.36	0.12	0.21	0.39	0.13	0.05	0.08	0.06	0.13	0.12
D3	0.20	0.58	0.29	0.31	0.11	0.01	0.36	0.02	1.34	0.56
10^5 PFU										
Class 0	−	−	−	−	0.07	0.01	−	+	0.02	−
Class 1	−	−	0.10	0.01	−	−	−	0.04	0.12	0.00
Class 1	0.00	−	−	0.00	−	−	0.17	0.06	0.02	0.03
Class 1	−	−	0.06	0.02	−	0.10	0.24	0.01	−	ND
Class 1	0.67	−	0.91	−	0.21	−	0.12	0.06	0.23	+
Class 3	−	−	0.14	−	0.01	−	−	+	−	−
E3	0.13	+	0.26	0.41	0.57	0.70	0.35	0.22	+	+
E5	1.73	+	5.26	−	0.03	0.35	3.52	0.38	+	1.42
D3	0.00	0.07	0.17	0.04	0.00	0.00	0.19	0.05	0.07	0.06
D3	0.19	0.39	ND	0.04	0.25	0.04	+	0.02	−	0.32

[a] Mice were injected i.p. with the indicated dose. Each row represents 1 of 10 individual mice at each dose. A plus or minus sign indicates the presence or absence, respectively, of MAV-1 DNA in each organ as determined by PCR amplification. Numbers indicate level of MAV-1 DNA normalized to the mouse rRNA gene as determined by dot blot hybridization for organs which were PCR positive for viral DNA.

[b] Class 0, mouse that had no signs. Class 1, mouse with class 1 signs: ruffled coat, hunched posture, rigid tail carriage, and lethargy. Class 2, mouse with class 2 signs: pauses in activity, crawling, hypermetria, and paraphimosis. Class 3, mouse with ≤2 class 3 signs: ataxia, burrowing into bedding, hyperreflexia, hyperesthesia, hyperpnea, and distended bladder. "E" designation, mouse with ≥3 class 3 signs or with class 4 signs: abdominal breathing, loss of righting reflex, paresis, and flaccid paralysis. "E" indicates that the mouse was euthanized, and the number indicates the day of euthanasia. "D" indicates that the mouse died, and the number indicates the day of death.

[c] ND, not determined.

[d] The two euthanized mice were tested for viral DNA in Peyer's patches; one mouse that died was tested for viral DNA in testes; all of these samples were positive.

histopathological manifestations of MAV-1 infection between the two strains.

Recently, i.p. injection of 6-week-old C57BL/6 mice with 10^4 PFU or DBA/2J mice with 5×10^3 PFU has been shown to result in 100% mortality by day 6 (5a). Clinically these inbred mice had signs of acute central nervous system disease including ataxia, tremor, seizures, and paralysis which were the results of a hemorrhagic encephalomyelitis. These results parallel the clinical signs and pathologic findings that we report here for adult outbred Swiss mice.

MAV-1-associated disease was comparable between the less susceptible CD-1 and the more susceptible NIHS mice for all criteria tested. The two differed only in the quantity of virus necessary to induce disease. Both strains of mice responded to MAV-1 infection by producing anti-MAV-1 serum antibodies. Although the level of the antibody response was not quanti-

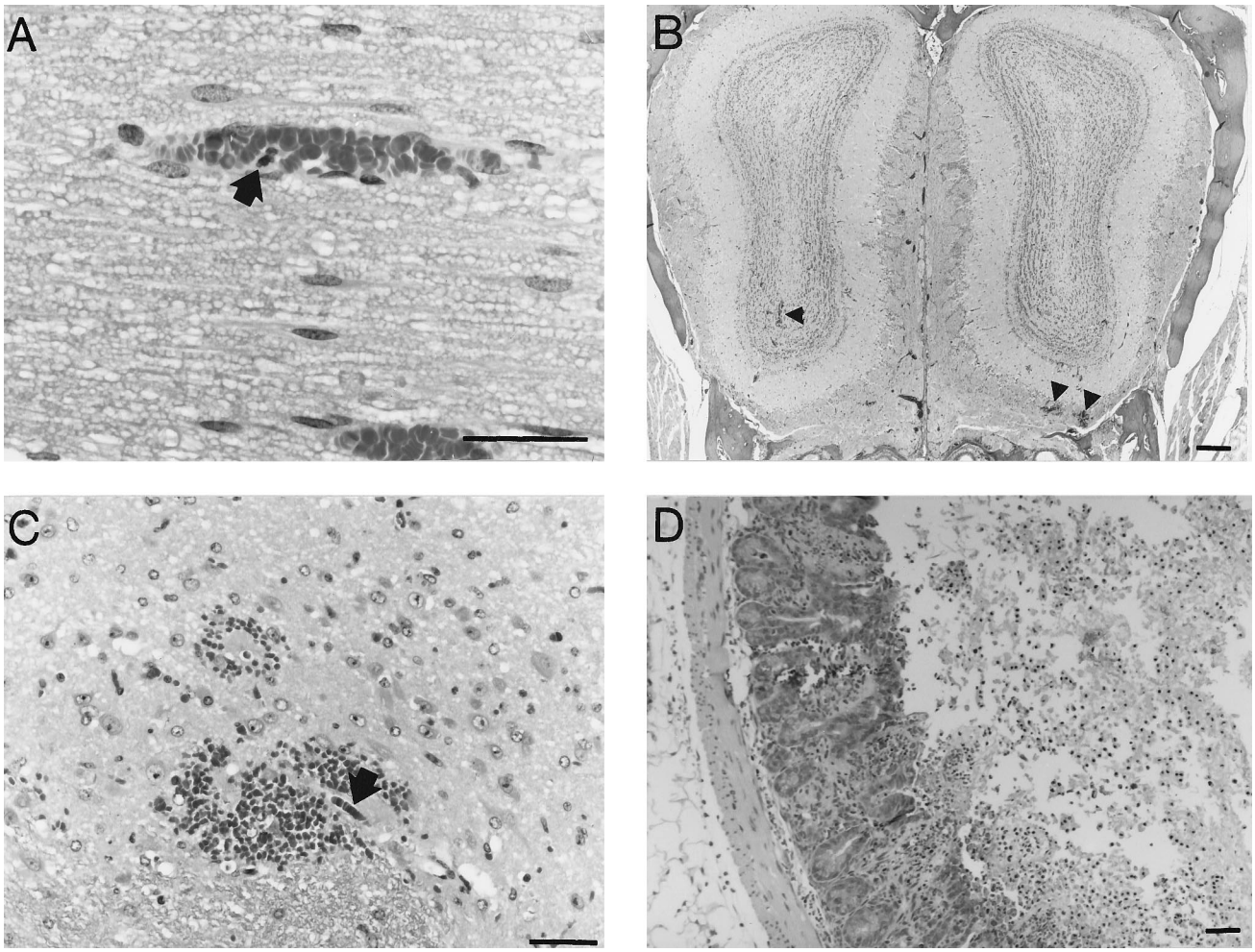

FIG. 1. Histopathological manifestations of MAV-1 infection of an NIHS mouse infected with 10 PFU. Similar results were seen with CD-1 mice (data not shown). (A) Endothelial necrosis in a small vein in the spinal cord; arrow indicates nucleus of endothelial cell which shows condensation of chromatin; the cell is bulging into vascular lumen, a prelude to eventual sloughing. (B) Multifocal petechial hemorrhages in white and gray matter of the brain; arrowheads indicate several of the more prominent hemorrhages. (C) A small focus of hemorrhage in the brain surrounding a capillary (arrow). (D) Segmental enteritis in the duodenum with severe necrosis and sloughing of the villar epithelium. The remaining mucosa and submucosa are filled with inflammatory cells. The intestinal lumen is filled with aggregates of sloughed epithelium, erythrocytes, and inflammatory cells. Bars, 0.7 μm (A, C, and D) or 7 μm (B).

tated, it seems likely that some other immune mechanism is responsible for clearance of MAV-1 or control of the infection. It will be interesting to investigate the mechanism controlling this susceptibility difference by studying inbred mouse strains and to determine if these susceptibility differences occur with other murine infectious agents.

We thank Kathy Davis for the preparation of histological sections and Abigail Smith for serological testing. We acknowledge Rich Meagher for the gift of the 18S rRNA gene probe.

This work was supported by NIH R01 AI23762 to K.R.S. K.R.S. is the recipient of an NIH Research Career Development Award.

REFERENCES

1. **Ball, A. O., and K. R. Spindler.** Unpublished data.
1a. **Beard, C. W., A. O. Ball, E. H. Wooley, and K. R. Spindler.** 1990. Transcription mapping of mouse adenovirus type 1 early region 3. Virology **175:**81–90.
2. **Blailock, Z. R., E. R. Rabin, and J. L. Melnick.** 1967. Adenovirus endocarditis in mice. Science **157:**69–70.
3. **Edmondson, D. G., and E. N. Olson.** 1989. A gene with homology to the myc similarity region of MyoD1 is expressed during myogenesis and is sufficient to activate the muscle differentiation program. Genes Dev. **3:**628–640.
4. **Ginder, D. R.** 1964. Increased susceptibility of mice infected with mouse adenovirus to Escherichia coli-induced pyelonephritis. J. Exp. Med. **120:** 1117–1128.
5. **Goidl, E. A., and G. W. Siskind.** 1974. Ontogeny of B-lymphocyte function: I. Restricted heterogeneity of the antibody response of B lymphocytes from neonatal and fetal mice. J. Exp. Med. **140:**1285–1302.
5a. **Guida, J. D., G. Fejer, L.-A. Pirofski, C. F. Brosnan, and M. S. Horwitz.** 1995. Mouse adenovirus type 1 causes a fatal hemorrhagic encephalomyelitis in adult C57BL/6 but not BALB/c mice. J. Virol. **69:**7674–7681.
6. **Hartley, J. W., and W. P. Rowe.** 1960. A new mouse virus apparently related to the adenovirus group. Virology **11:**645–647.
7. **Heck, F. C., Jr., W. G. Sheldon, and C. A. Gleiser.** 1972. Pathogenesis of experimentally produced mouse adenovirus infection in mice. Am. J. Vet. Res. **33:**841–846.
8. **Laird, P. W., A. Zijderveld, K. Linders, M. A. Rudnicki, R. Jaenisch, and A. Berns.** 1991. Simplified mammalian DNA isolation procedure. Nucleic Acids Res. **19:**4293.
9. **Margolis, G., L. Kilham, and E. M. Hoenig.** 1974. Experimental adenovirus infection of the mouse adrenal gland. I. Light microscopic observations. Am. J. Pathol. **75:**363–372.
10. **Pirofski, L., M. S. Horwitz, M. D. Scharff, and S. M. Factor.** 1991. Murine adenovirus infection of SCID mice induces hepatic lesions that resemble human Reye syndrome. Proc. Natl. Acad. Sci. USA **88:**4358–4362.
11. **Raviprakash, K. S., A. Grunhaus, M. A. El Kholy, and M. S. Horwitz.** 1989. The mouse adenovirus type 1 contains an unusual E3 region. J. Virol. **63:**5455–5458.
12. **Reed, L. J., and H. Muench.** 1938. A simple method of estimating fifty per

cent endpoints. Am. J. Hyg. **27:**493–497.
13. **Richter, C. B.** 1986. Mouse adenovirus, K virus, pneumonia virus of mice, p. 137–161. *In* P. N. Bhatt, R. O. Jacoby, H. C. I. Morse, and A. E. New (ed.), Viral and mycoplasmic infections of laboratory rodents: effects on biomedical research. Academic Press, New York.
14. **Riley, V., F. Lilly, E. Huerto, and D. Bardell.** 1960. Transmissible agent associated with 26 types of experimental mouse neoplasms. Science **132:**545–547.
14a. **Spindler, K. R.** Unpublished data.
15. **Torczynski, R., A. P. Bollon, and M. Fuke.** 1983. The complete nucleotide sequence of the rat 18S ribosomal RNA gene and its comparison with the respective yeast and frog genes. Nucleic Acids Res. **11:**4879–4890.
16. **Tyan, M. L.** 1968. Studies on the ontogeny of the mouse immune system: I. Cell-bound immunity. J. Immunol. **100:**535–542.
17. **van der Veen, J., and A. Mes.** 1973. Experimental infection with mouse adenovirus in adult mice. Arch. Gesamte Virusforsch. **42:**235–241.
18. **Wigand, R.** 1980. Age and susceptibility of swiss mice for mouse adenovirus, strain FL. Arch. Virol. **64:**349–358.
19. **Winters, A. L., and H. K. Brown.** 1980. Duodenal lesions associated with adenovirus infection in athymic "nude" mice. Proc. Soc. Exp. Biol. Med. **164:**280–286.
20. **Winters, A. L., H. K. Brown, and J. K. Carlson.** 1981. Interstitial pneumonia induced by a plaque-type variant of mouse adenovirus. Proc. Soc. Exp. Biol. Med. **167:**359–364.